**Bull. of Egyp. Soc. Physiol. Sci.**

(Official Journal of Egyptian Society for Physiological Sciences)

**(pISSN: 1110-0842; eISSN: 2356-9514)**

# Effect of Glucostasis on Extrapyramidal Dysfunction in Diabetic Rats

**Ahmad M Gaafar[a], Mohamed H Ahmed [a], Saly S Donia [a], Dina M Allam[b], Aya E Mohamed [a],Essam OHendya [a],**

a Department of Medical Physiology, Faculty of Medicine, Menoufia University, Egypt.

b Department of Pathology, Faculty of Medicine, Menoufia University, Egypt.

**Submit Date :** 7 Aug. 2025
**Revised Date** :31 Aug. 2025
**Accept Date :** 2 Sept. 2025

**Keywords**

- Glucostasis,
- Parkinson's disease
- Diabetes Mellitus
- L-DOPA and DDP4 inhibitor

**Abstract**

**Methods:** Fifty male Wistar albino rats were randomized into five equal groups: Control (C), Diabetic parkinsonian non-treated (D+P), L-DOPA/carbidopa treated diabetic parkinsonian (L/C D+P), vildagliptin/metformin-treated diabetic parkinsonian (V/M D+P), and vildagliptin/metformin & L-DOPA/carbidopa treated diabetic parkinsonian (V/M+L/C D+P). Diabetes was induced by a high-fat diet and streptozotocin, followed by rotenone to induce parkinsonism. Treatments were given orally for 3 weeks. Behavioral tests, glycemic indices, oxidative stress markers, dopamine levels, and histopathological/immunohistochemical analyses were assessed. **Results:** The D+P group showed hyperglycemia, insulin resistance, oxidative stress (↑MDA, ↑TNF-α, ↓GPX), reduced dopamine, impaired cognition and motor activity, and basal ganglia degeneration with ↑Bax/↓Bcl-2 expression. L/C D+P showed improved motor activity and dopamine, but did not correct glycemic or oxidative changes. V/M D+P showed improved glucostasis and oxidative markers, with partial restoration of dopamine and histology. The V/M+L/C D+P group showed the most comprehensive recovery, with normalization of glycemic indices, oxidative balance, dopamine, behavioral performance, and preservation of basal ganglia structure. **Conclusion:** Three weeks of combined vildagliptin, metformin, and L-DOPA produced synergistic neuroprotection in diabetic PD rats, suggesting that restoring glucostasis enhances L-DOPA efficacy and may represent a promising adjunctive therapeutic strategy.

**Corresponding author: Aya Eldesoky Mohamed**, **Mobile:** (+20)1000651539, **E-Mail:** aya.eldesoky91@yahoo.com

**Introduction**

Parkinson's disease (PD) is a progressive neurodegenerative disorder primarily characterized by motor symptoms such as bradykinesia, rigidity, resting tremors, and postural instability. These characteristics result from the disruption of the basal ganglia's circuitry due to the loss of dopaminergic neurons in the substantia nigra pars compacta [1]. Although the etiology of Parkinson's disease (PD) is still multifactorial, metabolic dysfunctions, particularly type 2 diabetes mellitus (T2DM), have drawn more attention as a possible component in the pathophysiology and progression of PD [2]. The central nervous system is significantly impacted by type 2 diabetes [3]. Accumulating clinical and experimental evidence suggests that individuals with T2DM have an increased risk of developing PD and may experience more rapid progression of both motor and cognitive deficits [4]. The connection between the two illnesses may be due to shared pathophysiological pathways, such as oxidative stress, persistent low-grade inflammation, mitochondrial dysfunction, and altered insulin signaling [2]. Specifically, the substantia nigra and striatum, two important brain areas involved in motor control, have high levels of insulin receptor expression [5]. Insulin resistance in the brain during diabetes may impede synaptic plasticity, interfere with dopaminergic neurotransmission, and encourage neuronal death. In diabetics, these changes may increase extrapyramidal dysfunction and resemble or worsen parkinsonian motor symptoms [6]. The gold standard for treating Parkinson's disease symptoms is levodopa (L-DOPA), which raises central dopamine levels but has no effect on metabolic dysfunction and may exacerbate oxidative stress. Additionally, L-DOPA may function as an anti-incretin, inhibiting the neuroprotective effects of glucagon-like peptide-1 (GLP-1) and increasing therapeutic resistance in certain Parkinson's disease patients [7]. Neuroprotection may result from pharmacologically restoring metabolic homeostasis [8]. As a first-line antidiabetic, metformin decreases oxidative stress, stimulates AMP-activated protein kinase (AMPK), and improves insulin sensitivity [5]. In diabetic and neurodegenerative models, vildagliptin, an inhibitor of dipeptidyl peptidase-4 (DPP-4), augments endogenous incretin activity, such as GLP-1, which has neurotrophic, anti-inflammatory, and anti-apoptotic properties [9]. Recent research has shown that the combination of metformin and vildagliptin not only enhances glycemic management but also reduces brain apoptosis and neuroinflammatory processes [10]. This combination increases the effectiveness of L-DOPA by improving central insulin signaling and regulating blood glucose (glucostasis). This alleviates extrapyramidal dysfunction in diabetic animals and presents a viable treatment approach that links metabolic management and neurodegeneration [11].

**2. MATERIALS AND METHODS**

The current study was conducted in the Medical Physiology Department of the Faculty of Medicine at Menoufia University in Egypt with approval from the ethical committee (N:3/2022PHYS43). The US National Institutes of Health's standard for the care and use of laboratory animals [12] was followed for the housing, handling, sampling, and experimental procedures of the animals.

**2.1. Animals and experimental groups.**

Figure (1) illustrates the experimental design's flow chart. A local animal supply facility provided fifty male Wistar albino rats, each weighing between 160 and 200 grams and aged two to three months. Three animals per cage were housed in fully ventilated cages (80 x 40 x 30 cm) with free access to water and a semi-synthetic balanced diet. The cages were kept at room temperature with an artificial 12-hour light/dark cycle. Rats were randomly assigned to five equal groups of ten rats each following two weeks of acclimatization.

**Group 1:** Control (C) group: rats with fasting blood glucose levels less than 110 mg/dl were selected in this group **[13].** Rats were injected intraperitoneally (I.P) by single dose of citrate buffer (Adwic, Egypt).; vehicle of streptozotocin (STZ), then injected subcutaneously with nine doses of sunflower oil; vehicle of rotenone (ROT) every 48 h (18 days), then continued with distilled water given by esophageal gavage once daily for 3 weeks (duration of treatment).

**Group 2:** Diabetic parkinsonian non-treated (D+P) group: Rats were given a high-fat diet (HFD) for four weeks, followed by a single intraperitoneal (I.P.) injection of 35 mg/kg of STZ (Sigma Chemical Company, USA). Three days following the STZ injection, diabetes was established. Rats with fasting blood glucose levels greater than 110-115 mg/dL using rat tail samples were classified as diabetics [14]. Following the creation of the diabetes model, a parkinsonian animal model was created by administering nine subcutaneous (s.c.) doses of rotenone (Sigma Aldrich, Egypt) at a dose of 1 mg/kg every 48 hours (18 days). Reducing the lethality of rotenone was the advantage of this regimen [15].

**Group 3:** L-DOPA/carbidopa-treated diabetic parkinsonian (L/C D+P) group: Rats were given Sinemet pills 100/25 levodopa/carbidopa in a dose of 12 mg/kg (Merck, Sharp and Dohme, S.p.A., Italy) crushed in water and administered by esophageal gavage [16] once daily for three weeks after the diabetes parkinsonian model was established.

**Group 4:** Vildagliptin/Metformin-treated diabetic parkinsonian (V/M D+P) group: Rats were given oral vildagliptin 3 mg/kg/day (Galvus, Novartis, Bangkok, Thailand) and metformin 30 mg/kg/day (Glucophage, Merkserono, Bangkok, Thailand) crushed in water via esophageal gavage for three weeks after the diabetes parkinsonian model was established [17].

**Group 5:** Vildagliptin/metformin and L-DOPA/carbidopa treated diabetic parkinsonian (V/M+L/C D+P) group: Rats were given the above-mentioned doses of metformin, vildagliptin, and L-DOPA/carbidopa for three weeks after the diabetes parkinsonian model was established. All of the groups' animals survived until the end of the experiment.

**2.2. Study design:**

All rats underwent neurobehavioral evaluation utilizing open field and Y-maze tests at the end of the ten-week experiment. Following measurements of insulin, HbA1c, and serum glucose, HOMA-IR was computed using the following formula: HOMA-IR = [fasting serum insulin (µIU/ml)]/405 [18]. Rats were sacrificed by cervical elongation and dislocation. After carefully removing the brains, ice-cold saline was used to wash them. The brains of the left hemisphere's basal ganglia were separated and homogenized. The homogenate underwent centrifugation. Tumor necrosis factor-α

(TNF-α), glutathione peroxidase (GPX), dopamine (DA), and malondialdehyde (MDA) were measured in the supernatants. The basal ganglia of the right hemisphere were prepared for histopathological and immunohistochemical studies. Animal remains were disposed of in a bio-secure and hygienic way.

**2.3. Assessment of behavior and spatial memory.**

**2.3.1. Open field test:** Every rat was positioned in the middle of an open field box measuring 1 m by 1 m by 50 cm, with a floor that was divided into squares measuring 20 cm by 20 cm. A silent room with regulated lighting was used to watch the rat's locomotor activity for five minutes after it was placed in the middle of the field. Between rats, 70% ethanol was used to wipe the box's floor. Latent duration, number of crossed squares, center crossing, rearing, and grooming were all measured with a digital video camera [19]. The rats were not given any prior instruction to encourage them to investigate the box.

**2.3.2. Y-maze:** The Y-maze's three arms, each measuring 60 cm in length, 11.5 cm in width, and 25 cm in height, were all composed of wood. For five minutes, each rat was positioned in the middle of the Y-maze to investigate it. When all four of the animal's paws were fully inside the Y-maze's arm, the entry was scored. Any three successive entries of the three separate arms were considered an alternation and were counted as correct choices. Rodents' innate propensity to choose different arms in a Y-maze on their own is known as spontaneous alternation, and it's regarded as a quick and easy test of spatial working memory [20]. By dividing the total number of alternations by the total number of choices less two, the percentage of spontaneous alternation (the ratio of right choices) was computed [21]. Between rats, 70% ethanol was used to wipe the box's floor.

**2.4. Biochemical assays**

Using tiny heparinized capillary tubes inserted into the medial epicanthus of the rats' eyelids, 3 milliliters of fasting blood samples were taken from the retro-orbital venous plexus of the rats at the conclusion of the experiment and following a neurological evaluation. For the purpose of estimating glycosylated hemoglobin (HbA1c), one milliliter was taken in an EDTA-containing tube. The remaining two milliliters were collected in a graduated centrifuge tube, allowed to clot for fifteen minutes at room temperature, and then centrifuged for fifteen minutes at 3000 r.p.m. [22]. The supernatant serum was collected in a dry, clean tube and kept at -20˚C until it was needed to measure insulin, glucose, Rats were then sacrificed by lengthening and then dislocating their necks. After carefully removing the brains, ice-cold saline was used to wash them. On an ice-cold glass plate, each brain was dissected. Glass rods were used to separate, weigh, and homogenize each brain's left hemisphere basal ganglia. In phosphate-buffered solution (PH=7), homogenization was performed at 10% (w/v). The homogenate underwent ten minutes of centrifugation at 2000×g. The supernatants were stored at -80°C until the levels of glutathione peroxidase (GPX), dopamine (DA), malondialdehyde (MDA), and tumor necrosis factor-α (TNF-α) were measured.

**2.5. Histopathological assessment of the brain tissue.**

**2.5.1. Histopathological examination:** After being stored in 10% buffered formalin and

dehydrated with varying alcohol concentrations, the brain was cleaned using xylol. Lastly, each of them was embedded separately in blocks of paraffin. After dewaxing, the 5-µm-thick tissue slices were stained with H&E. It was then examined under a light microscope to find any pathological changes [23]. A light microscope with 10, 20, 40, and 100× objectives was used to view the sections, and the following criteria were used to qualitatively classify pathological lesions in brain tissue: The following system was used to grade the pathological lesion severity: 0, no lesion; 1, mild lesion; 2, moderate lesion; and 3, severe lesion. This included inflammatory cell infiltration, necrosis, bleeding, oedema, degeneration, Lewis bodies, and gliosis. Pathological scores ranging from 0 to 3 were determined for all parameters, according to **[24].**

**2.5.2. Immunohistochemical staining and assessment:**

The streptavidin-biotin amplification technique was used for immunostaining, and diaminobenzidine (DAB) was the appropriate substrate/chromogen reagent. After that, the slides were rehydrated and dewaxed. Citrate buffer saline (pH 6) was boiled and then cooled to an average temperature in order to retrieve the antigen. The secondary antibody (Envision, FLEX, code 8002, Dako) was added after the primary antibody had been incubated at room temperature for the entire night. Mayer's hematoxylin was utilized as a counterstain and DAB was utilized as a chromogenic substrate. Positive controls were sections of normal rat pancreas and human tonsil, respectively. The two main antibodies used were against Bax (rabbit polyclonal antibody (Cat. no. bs-3010R; dilution 1:200), Bioss antibodies, USA), and Bcl2 (mouse monoclonal antibody (Cat. no. A20777; dilution 1:500), ABclonal, Life Science, USA). In every run, a slide devoid of the primary antibody served as a negative control. In positive cells, brownish cytoplasmic staining demonstrated Bcl-2 expression [25]. If any cells exhibited distinct staining, the case was deemed affirmative. The H-score was used to score the expression semi-quantitatively. The "H-score" was used to measure the degree of positive staining, with 0 representing no staining, 1 representing faintly brown, 2 representing substantially brown, and 3 representing dark brown. The proportion of cells that were favorably stained was calculated. Both figures were multiplied to determine the H-score [26].

**2.6. Statistical analysis.**

Version 22 of the SPSS software program (Statistical Package for the Social Science, SPSS Inc., Chicago, Illinois, USA) was used to analyze the data. The data were displayed as mean ± SD. A one-way analysis of variance (ANOVA) test with Tukey's post hoc test was used to compare quantitative variables between the groups under study. A difference was deemed statistically significant if p was less than 0.05. Fisher's exact tests are used in histological comparisons to illustrate the importance of the groups under study.

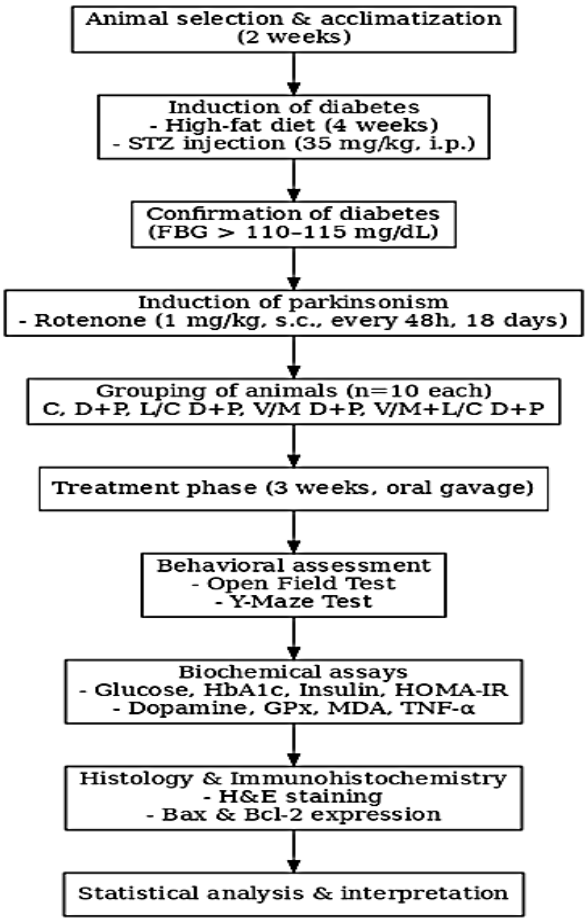


**Figure (1):** Flow chart of the experimental design

## 3. RESULTS

### 3.1. Cognitive and behavioral changes.

#### 3.1.1. Performance of open field test:

Figure (2[A, B, C, D, E]) demonstrates the performance in the open field test by all the studied groups. Latent period, number of squares crossed, center crossings, and frequency of rearing and grooming were significantly impaired ($P < 0.001$) in the D+P group compared to the C group. These parameters were significantly improved ($P < 0.001$) in both the L/C D+P and V/M D+P groups compared to the D+P group, with greater improvement ($P < 0.001$) observed in the L/C D+P group than in the V/M D+P group. In the V/M+L/C D+P group, all parameters showed no significant difference ($P > 0.05$), when compared to the C group.

3.1.2. Performance of Y-Maze test:

Figure (2[F]) illustrates the performance in the Y-maze test by all the studied groups. The percentage of spontaneous alternations was significantly decreased ($P <0.001$) in the D+P and L/C D+P groups compared to the C group, with no significant difference ($P > 0.05$) observed between the D+P and L/C D+P groups. In contrast, the V/M D+P and V/M+L/C D+P groups showed significantly higher percentages of spontaneous alternations ($P < 0.001$) than both the D+P and L/C D+P groups, with no significant difference ($P > 0.05$) compared to the C group.

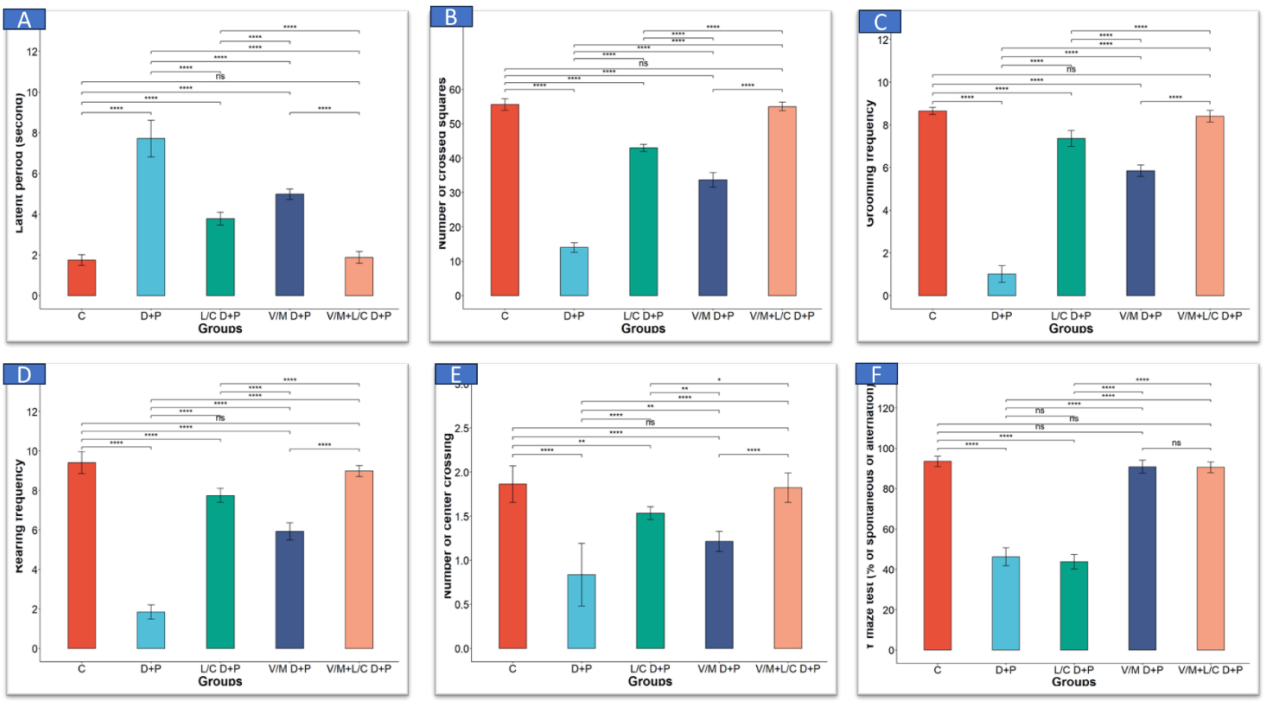


**Figure (2): Open field test**, latent period [A], Number of crossed squares [B], Grooming frequency[C], Rearing frequency [D] , Number of crossed squares [E], and Y- maze tests among the studied groups.

### 3.2. Changes of dopamine level

Figure (3[A]) demonstrates the difference in mean ± SD of dopamine **(**DA)level in the brain tissue homogenates of the different studied groups.

Dopamine (DA) level in the D+P group showed a significant decrease (P <0.001) when compared to that of the C group. In L/C D+P, V/M D+P, and V/M+L/C D+P groups, DA levels were significantly increased (P < 0.001) when compared with those of the D+P group. In the L/C D+P group, DA level was significantly higher (P < 0.001) than that of V/M D+P, and there was an insignificant change (P > 0.05) between V/M+L/C D+P and C groups.

### 3.3. Changes of oxidative stress and inflammatory markers

Figure (3[B, C, D]) demonstrates the difference in mean ± SD of enzymatic activity of GPX, MDA level, and TNF-α in the brain tissue homogenates of the different studied groups.

There were significant (↑MDA, ↑TNF-α) and (↓GPX) levels (P < 0.001) in D+P and L/C D+P groups when compared to those of the C group, and insignificant change (P > 0.05) between D+P and L/C D+P groups. In V/M D+P and V/M+L/C D+P groups, there was a significant (↓MDA, ↓TNF-α) and (↑GPX) levels (P < 0.001) when compared with those of the D+P group and L/C D+P. Also, in the V/M+L/C D+P group, MDA, TNF-α, and GPX levels were insignificantly changed (P > 0.05) when compared with those of the C group.

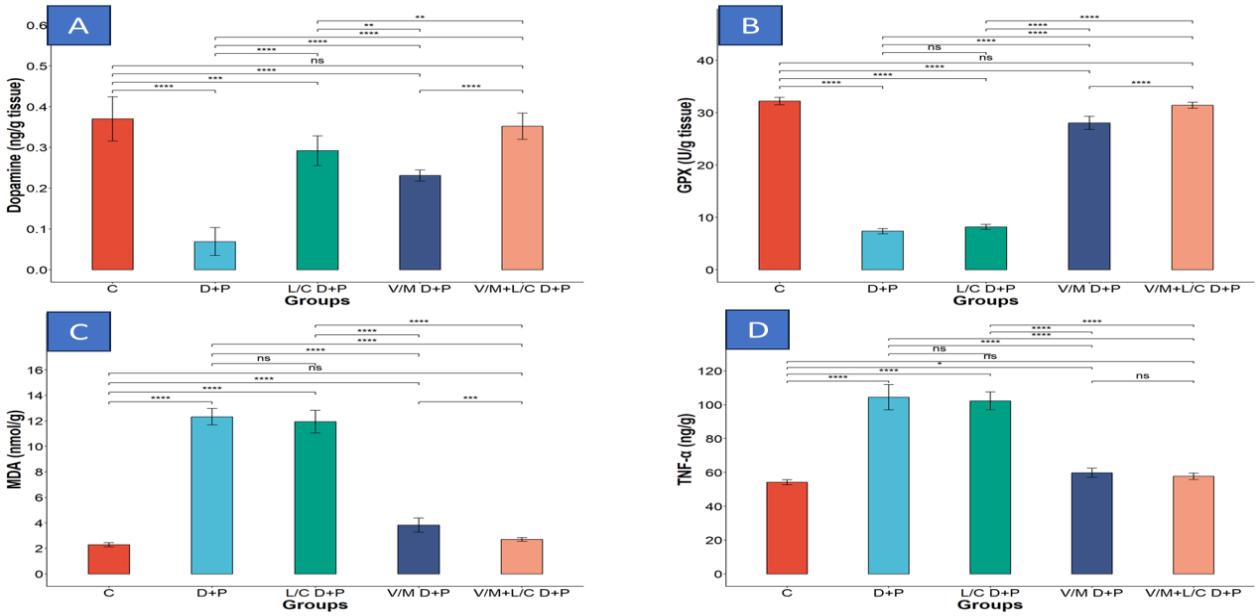


**Figure (3):** Dopamine [A], Glutathione peroxidase (GPX, [B]), Malondialdehyde (MDA, [C]), Tumor necrosis factor-alpha (TNF-α, [D]) in the studied groups.

### 3.4. Glycemic state

Table (1) shows the difference in mean ± SD of fasting serum glucose, HbA1c, insulin and HOMA-IR index of the different studied groups. There was a significant increase ($P < 0.001$) in these parameters in the D+P and L/C D+P groups when compared to the C group, and there was a non-significant change ($P > 0.05$) between D+P and L/C D+P groups. In V/M D+P and V/M+L/C D+P groups, these parameters were significantly decreased ($P < 0.001$) when compared to those of D+P and L/C D+P groups. Also, in the V/M+L/C D+P group, these parameters were insignificantly changed ($P > 0.05$) when compared to those of the C group.

**Table (1): Fasting serum glucose, HbA1c, Insulin and HOMA IR index in the studied groups**

| Groups / Parameter | C | D+P | L/C D+P | V/M D+P | V/M+L/C D+P |
|---|---|---|---|---|---|
| Fasting serum glucose (mg/dl) | 93.92 ± 1.183 | 396.07 ± 9.397* | 400.57 ± 5.504* | 96.22 ± 1.487#$ | 96.73 ± 1.143#$ |
| HbA1c (% of normal) | 5.38 ± 0.187 | 9.75 ± 0.585* | 10.07 ± 0.386* | 5.79 ± 0.403#$ | 5.81 ± 0.229#$ |
| Insulin (uIU/ml) | 12.88 ± 0.394 | 16.08 ± 0.109* | 16.35 ± 0.148* | 12.98 ± 0.127#$ | 13.16 ± 0.586#$ |
| HOMA-IR index | 3.07 ± 0.091 | 6.62 ± 0.968* | 6.85 ± 0.188* | 3.14 ± 0.066#$ | 3.20 ± 0.062#$ |

Data are expressed as mean ± standard deviations. Number of rats in each group was ten (n=10). One way analysis of variance with Tukey's post-hoc test was applied, and significant level was set on $P \leq .05$. The marks *, # and $ indicates significant differences, when are compared with the corresponding values of C, D+P and L/C D+P groups, respectively.

### 3.5. Histopathological examination.

#### 3.5.1. Hematoxylin and eosin-stained sections.

In the C group, normal appearance was found (vesicular nuclei, prominent nucleoli, and scant rim of basophilic cytoplasm) without any histopathological changes.

The D+P group revealed marked histological changes in the form of strong inflammatory infiltrates, degenerative changes, perivascular oedema, severe gliosis, and acidophilic Lewis bodies.

In the L/C D+P group, there was mild improvement of the histological picture, where moderate inflammatory cells, moderate neurodegenerative changes, moderate degree of gliosis, and edema. In the V/M D+P group, there was a moderate improvement of the histological picture; mild inflammatory infiltrates, mild neurodegenerative changes, and mild oedema.

V/M+L/C D+P group showed a marked regression of inflammation with restoration of the normal histological picture.

Table (2) shows a comparison of the percentages of the histopathological changes in the basal ganglia (lymphocytic infiltration, gliosis, degenerative changes, edema, necrosis and Lewis bodies) in all the studied groups.

There was a statistically significant difference ($P < 0.001$) in lymphocytic infiltration, gliosis, degenerative changes, edema, necrosis, and Lewis bodies among the C, D+P, L/C D+P, V/M D+P, and V/M+L/C D+P groups. All rats (100%) in the C group exhibited no signs of lymphocytic infiltration, gliosis, degenerative changes, edema, necrosis, or Lewis bodies. In contrast, all rats (100%) in the D+P group showed severe lymphocytic infiltration, pronounced gliosis, marked degenerative changes, edema, necrosis, and the presence of Lewis bodies. Among the treated groups, the V/M+L/C D+P group demonstrated the most notable histopathological improvement, with the complete absence of all pathological features. Figure (4[A, B]) illustrates the histopathological changes (H&E) observed in the D+P and V/M+L/C D+P groups.

#### 3.5.2. Immunohistochemistry studies.

Table (2) shows the difference in mean ± SD of Bax and Bcl2 expression of the different studied groups.

In the D+P group, there was a significant (↑Bax and ↓ Bcl2) expression ($P < 0.001$) when compared to those of the C group. In L/C D+P and V/M D+P groups, there was a significant (↓Bax and ↑Bcl2) expression($P < 0.001$) when compared to D+P group, but there was a significant (↓Bax and ↑Bcl2) expressions($P < 0.001$) in V/M D+P when compared to L/C D+P group, In V/M+ L/C D+P group there was a significant (↓Bax ) expression($P < 0.001$) when compared to all groups, and significant (↑Bcl2) ($P < 0.001$) when compared to D+P and L/C D+P groups but insignificantly changed ($P > 0.05$) when compared to C and V/M D+P groups. Figure (4[C, D, E, F]) demonstrate Bax & (3[E, F]) demonstrates Bcl2 expressions in D+P and V/M+ L/C D+P groups.

**Table (2)** Comparison of the percentages of histopathological changes in the basal ganglia, mean ± SD of Bax and Bcl2 expression in the studied groups, showing the significance between the studied groups, The marks *, # , $ and & indicates significant differences, when are compared with the corresponding values of C, D+P , L/C D+P and V/M D+P groups respectively.

| Groups / Parameter | C | D+P | L/C D+P | V/M D+P | V/M+L/C D+P |
|---|---|---|---|---|---|
| Lymphocytic infiltration | | | | | |
| Negative | 10 (100.0) | - | - | 6 (60.0) #$ | 9 (90.0) #$ |
| Mild | - | - | - | 4 (40.0) #$ | 1 (10.0) #$ |
| Moderate | - | - | 2 (20.0) * | - | - |
| Strong | - | 10 (100.0) * | 8 (80.0) * | - | - |
| Gliosis | | | | | |
| Negative | 10 (100.0) | - | - | 6 (60.0) #$ | 8 (80.0) #$ |
| Mild | - | - | - | 3 (30.0) #$ | 2 (20.0) #$ |
| Moderate | - | - | 3 (30.0) * | 1 (10.0) #$ | - |
| Strong | - | 10 (100.0) * | 7 (70.0) * | - | - |
| Deg. Changes | | | | | |
| Negative | 10 (100.0) | - | - | 3 (30.0) *#$ | 9 (90.0) #$& |
| Mild | - | - | 1 (10.0) *# | 6 (60.0) *#$ | 1 (10.0) #$& |
| Moderate | - | - | 4 (40.0) *# | 1 (10.0) *#$ | - |
| Strong | - | 10 (100.0) * | 5 (50.0) *# | - | - |
| Edema | | | | | |
| Negative | 10 (100.0) | - | - | 5 (50.0) *#$ | 7 (70.0) #$ |
| Mild | - | - | - | 5 (50.0) *#$ | 3 (30.0) #$ |
| Moderate | - | - | 3 (30.0) * | - | - |
| Strong | - | 10 (100.0) * | 7 (70.0) * | - | - |
| Necrosis | | | | | |
| Negative | 10 (100.0) | - | - | 2 (20.0) *#$ | 8 (80.0) #$& |
| Mild | - | - | 2 (20.0) *# | 7 (70.0) *#$ | 2 (20.0) #$& |
| Moderate | - | - | 4 (40.0) *# | 1 (10.0) *#$ | - |
| Strong | - | 10 (100.0) * | 4 (40.0) *# | - | - |
| Lewis bodies | | | | | |
| Negative | 10 (100.0) | - | 1 (10.0) * | 7 (70.0) #$ | 9 (90.0) #$ |
| Positive | - | 10 (100.0) * | 9 (90.0) * | 3 (30.0) #$ | 1 (10.0) #$ |
| Bax expression | 0.00 ± 0.000 | 267.90 ±13.892* | 204.00 ±12.649*# | 50.00 ± 8.165 *#$ | 17.00 ±6.749*#$& |
| Bcl2 expression | 128.00 ± 13.166 | 0.00 ± 0.000 * | 30.00 ± 11.547*# | 106.00 ±18.974*#$ | 119.00 ±21.318#$ |

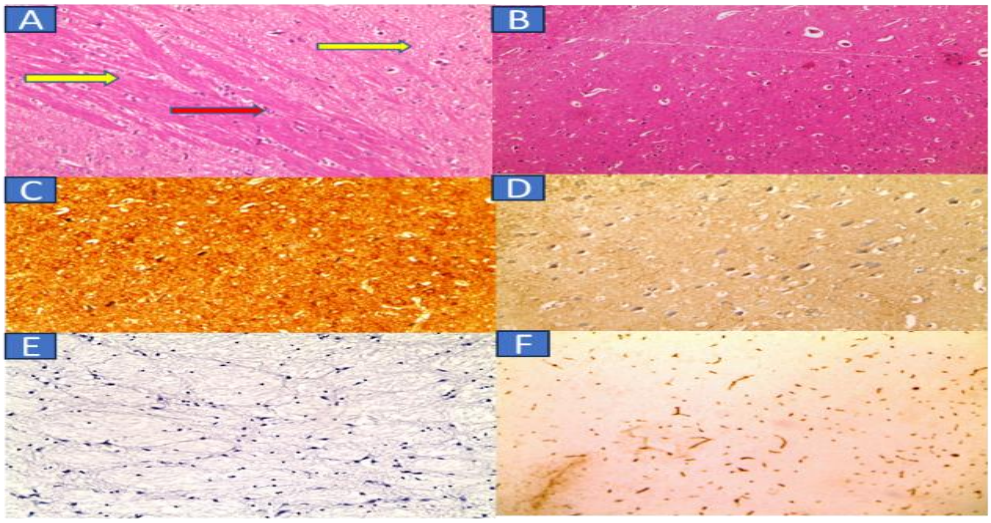


**Figure (4):** Section (H&E stain x100) of basal ganglia of ( D+P group) showing strong inflammatory reaction, lymphocytic infiltrates (red arrow), degenerative changes and perivascular oedema (yellow arrow) [A],Restoration of the normal picture of basal ganglia in V/M+ L/C D+P group [B]. Immunostaining of Bax in D+P group showing strong expression of Bax [C], and negative expression of Bcl2 [E], decreased expression of Bax [D], and increased expression of Bcl2 in V/M+ L/C D+P group.

## 4. DISCUSSION

In the present study, the D+P group showed significantly elevated fasting glucose, HbA1c, insulin, and HOMA-IR compared to controls after 10 weeks, confirming the development of insulin resistance and hyperglycemia. This is explained by partial β-cell damage induced by low-dose STZ and high-fat diet, causing progressive β-cell dysfunction and inflammation, resembling T2DM pathogenesis **[17].** The increased insulin and HOMA-IR reflect early β-cell compensation for systemic insulin resistance **[13],** but chronic oxidative stress and mitochondrial dysfunction eventually impair insulin secretion **[27].**

Consistent with our findings, **Rolo et al. [28]** reported that rotenone aggravates hyperglycemia through mitochondrial dysfunction and impaired insulin signaling.

Three weeks of L-DOPA/carbidopa therapy in the L/C D+P group did not improve glycemic indices compared to D+P, indicating persistence of insulin resistance. **Muthuraman et al. [29]** similarly reported that L-DOPA improves motor symptoms but not metabolic dysfunction. By contrast, three weeks of vildagliptin/metformin therapy (V/M D+P) significantly improved glycemic parameters, reflecting metformin's suppression of hepatic gluconeogenesis and enhancement of glucose uptake **[30]** and vildagliptin's prevention of incretin degradation, enhancing GLP-1 and GIP activity **[31].Dutta et al. [32]** supported our findings and explained that metformin improves insulin sensitivity.

Oxidative stress was significantly aggravated in the D+P group, as evidenced by elevated MDA and reduced GPX, findings consistent with hyperglycemia-induced ROS generation through pathways such as aldose reductase, advanced glycation, and mitochondrial overproduction of superoxide **[33,32].**L-DOPA/carbidopa treatment failed to correct these alterations, likely due to persistent hyperglycemia and ROS generated during dopamine metabolism, a phenomenon reported to exacerbate oxidative imbalance and dopaminergic toxicity **[11,35].** In contrast, three weeks of vildagliptin/metformin treatment significantly reduced MDA and increased GPX activity. This agrees with previous studies showing that metformin preserves mitochondrial function, reduces ROS production, and improves antioxidant defenses **[29],** while vildagliptin enhances GLP-1 signaling, which exerts antioxidant and neuroprotective effects **[9,10,46].** The combination therapy (V/M+L/C D+P) produced the most pronounced antioxidant effect, consistent with evidence that metabolic correction improves L-DOPA utilization and minimizes its oxidative side effects **[11,25].**

Inflammation paralleled these changes: TNF-α was elevated in D+P rats, explained by rotenone-induced microglial activation and insulin resistance via PI3K/Akt and NF-κB pathways **[34],** compounded by HFD-induced upregulation of inflammatory genes [35]. L-DOPA/carbidopa did not reduce TNF-α, consistent with **Del-Bel et al. [7],** who showed that L-DOPA activates neuron–microglia-astrocyte interactions. **Ward et al. [36]** also noted that dopamine metabolism generates ROS, further driving inflammation. Conversely, three weeks of vildagliptin/metformin reduced TNF-α significantly, consistent with **Al-Kuraishy et al. [10],** who demonstrated that metformin modulates astrocyte activity via AMPK and vildagliptin enhances GLP-1 signaling, which exerts anti-inflammatory effects **[37].**

Dopamine levels in the basal ganglia were markedly reduced in D+P rats, consistent with rotenone-induced mitochondrial complex I inhibition and neurodegeneration **[38,39].** This effect was aggravated by diabetes-related insulin resistance and mitochondrial dysfunction **[6],** consistent with **Bittencourt et al. [40],** who found reduced dopamine in HFD+STZ rats. L-DOPA/carbidopa restored dopamine **[29],** while vildagliptin/metformin also improved dopamine via mitochondrial protection and reduced apoptosis **[9,18].** The three-week combination

therapy normalized dopamine to near-control levels, showing synergistic benefit.

Behavioral results reflected these biochemical changes. In the open field, D+P rats had longer latency, reduced locomotion, and less rearing and grooming, consistent with dopamine depletion and oxidative stress **[41,42].** L-DOPA improved motor function by replenishing dopamine **[25],** while vildagliptin/metformin improved exploratory behavior via reduced oxidative stress and TNF-α, and enhanced GLP-1 neuroprotection **[8,9].Rout et al. [8]** reported that GLP-1 signaling protects dopaminergic neurons from degeneration and increases tyrosine hydroxylase expression, while metformin activates AMPK, promoting mitochondrial function and neuronal survival. The combination (V/M+L/C D+P) produced the greatest improvements, suggesting synergistic effects targeting both metabolic and dopaminergic deficits.

Cognitive function (Y-maze) declined in D+P rats due to dopaminergic loss and hippocampal insulin resistance, disrupting plasticity **[3,43].** L-DOPA did not improve alternation percentage, reflecting its limited effect on memory **[1,2]. Booth [1]** explained that L-DOPA primarily increases dopamine in the striatum (motor control), but has a limited effect in the prefrontal cortex or hippocampus, which are essential for working memory, cognition, and decision making. Vildagliptin/metformin improved cognitive performance, consistent with studies showing GLP-1 analogs improve cognition **[9,44].** Addition of L-DOPA did not enhance cognition beyond V/M alone, suggesting cognitive improvement depends more on metabolic and anti-inflammatory actions.

Histopathology confirmed severe degeneration, inflammation, and Lewis body formation in D+P rats **[38].** L-DOPA treatment provided only partial improvement, consistent with reports that dopaminergic replacement does not address neuroinflammation **[45].** Vildagliptin/metformin markedly reduced gliosis, edema, necrosis, and Lewis bodies, consistent with anti-inflammatory and mitochondrial protective effects **[46].** Combination therapy preserved basal ganglia architecture, suggesting complementary mechanisms.

Immunohistochemistry revealed upregulated Bax and downregulated Bcl-2 in D+P rats, consistent with oxidative stress and mitochondrial apoptosis **[23].** L-DOPA modestly reduced Bax without restoring Bcl-2, reflecting limited anti-apoptotic effects **[47].** Vildagliptin/metformin reduced Bax and increased Bcl-2, consistent with previous findings on mitochondrial protection and improved insulin signaling **[48].** The combination produced the strongest anti-apoptotic effect, confirming synergistic neuroprotection.

The present findings imply that correcting glucostasis with vildagliptin and metformin not only improves diabetic status but also enhances the therapeutic efficacy of L-DOPA in parkinsonism by targeting oxidative stress, inflammation, and apoptosis, these agents extend neuroprotection beyond dopaminergic replacement, which may translate into better control of motor and non-motor symptoms, improved quality of life, and slower disease progression in patients with diabetes-associated Parkinson's disease.

## 5. LIMITATIONS OF THE STUDY:

A limitation of the present study is that genetic aspects were not investigated due to financial constraints, which may provide deeper insights into the molecular mechanisms linking diabetes and Parkinson's disease. In addition, different doses and treatment durations of L-DOPA, metformin and vildagliptin were not explored, which could influence their efficacy and safety.

## 6. CONCLUSION:

Three weeks of vildagliptin and metformin administration, particularly in combination with L-DOPA, effectively restored glucostasis, alleviated oxidative stress and apoptosis, and improved behavioral and histological outcomes in diabetic Parkinsonian rats. These results highlight the importance of addressing metabolic dysfunction in Parkinson's disease and suggest that adjunctive use of antidiabetic agents may enhance L-DOPA efficacy and provide a novel therapeutic strategy for managing patients with comorbid diabetes and Parkinsonism.

## 7. REFERENCES


1. **Booth S.** Limitations in effective treatment of Parkinson's Disease: neuroanatomical substrate of L-DOPA induced dyskinesia and cognitive impairment. 2024.
2. **Ribarič S.** The contribution of type 2 diabetes to Parkinson's disease aetiology. Int J Mol Sci. 25:4358, 2024.
3. **Kakoty V, Kc S, Kumari S, Yang CH, Dubey SK, Sahebkar A, et al.** Brain insulin resistance linked Alzheimer's and Parkinson's disease pathology: an undying implication of epigenetic and autophagy modulation. Inflammopharmacology. 31(2):699–716, 2023.
4. **Dhyani S, Butola M, Sautha V, Jakhmola V.** Recent advances in treatment approaches for diabetes mellitus and related complications: a review. Int J App Pharm. 17(2):12–30, 2025.
5. **Li N, Zhou T, Fei E.** Actions of metformin in the brain: a new perspective of metformin treatments in related neurological disorders. Int J Mol Sci. 23(15):8281, 2022.
6. **Pérez-Taboada I, Alberquilla S, Martín ED, Anand R, Vietti-Michelina S, Tebeka NN, et al.** Diabetes causes dysfunctional dopamine neurotransmission favoring nigrostriatal degeneration in mice. Mov Disord. 35(9):1636–1648, 2020.
7. **Del-Bel E, Bortolanza M, Dos-Santos-Pereira M, Bariotto K, Raisman-Vozari R.** L-DOPA-induced dyskinesia in Parkinson's disease: are neuroinflammation and astrocytes key elements? Synapse. 70:479–500, 2016.
8. **Rout M, Prusty SK, Kar DM.** Therapies using anti-diabetics to prevent and manage progression of Parkinson's disease. Curr Drug Ther. 20(3):298–314, 2025.
9. **Pariyar R, Bastola T, Lee DH, Seo J.** Neuroprotective effects of the DPP4 inhibitor vildagliptin in in vivo and in vitro models of Parkinson's disease. Int J Mol Sci. 23(4), 2022.
10. **Al-Kuraishy HM, Sami OM, Hussain NR, Al-Gareeb AI.** Metformin and/or vildagliptin mitigate type II diabetes mellitus induced-

oxidative stress: the intriguing effect. J Adv Pharm Technol Res. 11(3):142–147, 2020.

11. **Lisco G, De Tullio A, Iovino M, Disoteo O, Guastamacchia E, Giagulli VA, Triggiani V.** Dopamine in the regulation of glucose homeostasis, pathogenesis of type 2 diabetes, and chronic conditions of impaired dopamine activity/metabolism: implication for pathophysiological and therapeutic purposes. Biomedicines. 11(11):2993, 2023.

12. **Garber JC, Barbee RW, Bielitzki JT, Clayton LA, Donovan JC, Hendriksen CFM, et al.** Guide for the care and use of laboratory animals: Institute for Laboratory Animal Research, Division on Earth and Life Studies. Washington DC, USA: National Academies Press; eighth. 220 p, 2011.

13. **Ahmed HH, Abd El-Maksoud MD, Abdel Moneim AE, Aglan HA.** Pre-clinical study for the antidiabetic potential of selenium nanoparticles. Biol Trace Elem Res. 177:267–280, 2017.

14. **Oztürk Z, Gurpinar T, Vural K, Boyacıoglu S, Korkmaz M, Var A.** Effects of selenium on endothelial dysfunction and metabolic profile in low dose streptozotocin induced diabetic rats fed a high fat diet. Biotechnic & Histochemistry. 90:506–515, 2015.

15. **El-Ghaiesh SH, Bahr HI, Ibrahiem AT, Ghorab D, Alomar SY, Farag NE, Zaitone SA.** Metformin protects from rotenone–induced nigrostriatal neuronal death in adult mice by activating AMPK-FOXO3 signaling and mitigation of angiogenesis. *Front Mol Neurosci*. 13:84, 2020.

16. **Carvalho MM, Campos FL, Marques M, Soares-Cunha C, Kokras N, Dalla C, et al.**Effect of levodopa on reward and impulsivity in a rat model of Parkinson's disease. FrontBehav Neurosci. 11:145, 2017.

17. **Apaijai N, Chinda K, Palee S, Chattipakorn S, and Chattipakorn N.** Combined vildagliptin and metformin exert better cardioprotection than monotherapy against ischemia-reperfusion injury in obese-insulin resistant rats. *PLoS One* 9: e102374, 2014.

18. **Matthews DR, Hosker JP, Rudenski AS, Naylor B, Treacher DF, and Turner R**. Homeostasis model assessment: insulin resistance and β-cell function from fasting plasma glucose and insulin concentrations in man. *diabetologia* 28: 412–419, 1985.

19. **Aksu I, Baykara B, Ozbal S, Cetin F, Sisman AR, Dayi A, et al.** Maternal treadmill exercise during pregnancy decreases anxiety and increases prefrontal cortex VEGF and BDNF levels of rat pups in early and late periods of life. Neuroscience Letters. 516:221–225, 2012.

20. **Arai K, Matsuki N, Ikegaya Y, Nishiyama N.** Deterioration of spatial learning performances in lipopolysaccharide-treated mice. Japanese Journal of Pharmacology. 3:195–201, 2001.

21. **Casadesus G, Milliken EL, Webber KM, Bowen RL, Lei Z, Rao CV, et al.** Increases in luteinizing hormone are associated with

declines in cognitive performance. Molecular and Cellular Endocrinology. 269:107–111, 2007.

22. **Schermer S.** Rats haemopoietic system. Blood morphology of laboratory animals.Chap. 10. Pb1 Davis FA Co, Philadelphia. 112, 1968.

23. **Yahia SH, Etewa SE, Saleh NS, Mohammad SM, Aboulfotouh NI, Kandil AM, Sarhan MH.** Histopathological, immunohistochemical and biochemical studies of murine hepato-splenic tissues affected by chronic toxoplasmosis. J Parasitol Res. 16:2165205, 2022.

24. **Evangelista FF, de Laet Sant'Ana P, Ferreira WC, Ferreira TA, Dos Santos ML, de Souza AH, de Andrade FAL, da Silva DA, de Barros LD, Colli CM, Nogueira-Melo GA, Costa IN, Falavigna-Guilherme AL.** The Brazilian Toxoplasma gondii strain BRI caused greater inflammation and impairment in anxiogenic behavior in mice, which was reverted by rosuvastatin treatment. Parasitol Res. 123:64, 2023.

25. **Wahba AS, Wahba NS, Sayed GA, Hamed SK, Abo-Elmatty DM, Mesbah NM, Reda AM.** Combined neuroprotective potential of vitamin E and levodopa/carbidopa in a rat model of rotenone-induced Parkinson's disease: role of AMPK/SIRT1/PGC-1α and HMGB1/RAGE axes. J Pharm Pharmacol. rgaf044, 2025.

26. **Numata M, Morinaga S, Watanabe T, Tamagawa H, Yamamoto N, Shiozawa M, Nakamura Y, Kameda Y, Okawa S, Rino Y, Akaike M, Masuda M, Miyagi Y.** The clinical significance of SWI/SNF complex in pancreatic cancer. Int J Oncol. 42:403–10, 2013.

27. **Gonzalez CD, Lee MS, Marchetti P, Pietropaolo M, Towns R, Vaccaro MI, Watada H, Wiley JW.** The emerging role of autophagy in the pathophysiology of diabetes mellitus. Autophagy. 7:2–11, 2011.

28. **Rolo AP, Palmeira CM.** Diabetes and mitochondrial function: role of hyperglycemia and oxidative stress. Toxicol Appl Pharmacol. 212(2):167–178, 2006.

29. **Muthuraman M, Koirala N, Ciolac D, Pintea B, Glaser M, Groppa S, et al.**Deep brain stimulation and L-DOPA therapy: concepts of action and clinical applications in Parkinson's disease. Front Neurol. 9:711, 2018.

30. **Natali A, Ferrannini E.** Effects of metformin and thiazolidinediones on suppression of hepatic glucose production and stimulation of glucose uptake in type 2 diabetes: a systematic review. Diabetologia. 49:434–441, 2006.

31. **Bukhari YA, Ghamdi FAR, Almuafi OS, Alzahrani AKJ, Alshamrani MAM, Alshehri SMO, et al.** Mechanism of action of vildagliptin and its role in type 2 diabetes management. J Int Crisis Risk Commun Res. 7(S6):1486, 2024.

32. **Dutta S, Shah RB, Singhal S, Dutta SB, Bansal S, Sinha S, Haque M.** Metformin: A review of potential mechanism and therapeutic

utility beyond diabetes. Drug Des Devel Ther. 17:1907–1932, 2023.

33. **Maheshwari R, Balaraman R, Sen AK, Shukla D, Seth A.** Effect of concomitant administration of coenzyme Q10 with sitagliptin on experimentally induced diabetic nephropathy in rats. Ren Fail. 39(1):130–139, 2017.

34. **Szukiewicz D.** Molecular mechanisms for the vicious cycle between insulin resistance and the inflammatory response in obesity. Int J Mol Sci. 24(12):9818, 2023.

35. **Moraes RC, Blondet A, Birkenkamp-Demtroeder K, Tirard J, Orntoft TF, Gertler A, Durand P, Naville D, Bégeot M.** Study of the alteration of gene expression in adipose tissue of diet-induced obese mice by microarray and reverse transcription-polymerase chain reaction analyses. Endocrinology. 144:4773–4782, 2003.

36. **Ward RJ, Dexter DT, Martin-Bastida A, Crichton RR.** Is chelation therapy a potential treatment for Parkinson's disease? Int J Mol Sci. 22(7):3338, 2021.

37. **Yin R, Xu Y, Wang X, Yang L, Zhao D.** Role of dipeptidyl peptidase 4 inhibitors in antidiabetic treatment. Molecules. 27(10):3055, 2022**.**

38. **Betarbet R, Sherer TB, MacKenzie G, Garcia-Osuna M, Panov AV, Greenamyre JT.**Chronic systemic pesticide exposure reproduces features of Parkinson's disease. Nat Neurosci. 3:1301–6, 2000.

39. **Fernandes EJ, Poetini MR, Barrientos MS, Bortolotto VC, Araujo SM, Santos Musachio EA, et al.** Exposure to lutein-loaded nanoparticles attenuates Parkinson's model-induced damage in Drosophila melanogaster: Restoration of the dopaminergic and cholinergic system and oxidative stress indicators. Chem Biol Interact. 340:109431, 2021.

40. **Bittencourt A, Brum PO, Ribeiro CT, Gasparotto J, Bortolin RC, de Vargas AR, et al.** High fat diet-induced obesity causes a reduction in brain tyrosine hydroxylase levels and non-motor features in rats through metabolic dysfunction, neuroinflammation and oxidative stress.

41. **Petschner T, Hofman K, Chen JZ, Andreska T, Wolf D, Knorr S, et al.** Chronic subthalamic nucleus deep brain stimulation reduces pathological TrkB aggregates in a Parkinson's disease rat model. Transl Neurodegener. 14(1):11, 2025.

42. **Zhao Y, Wang D, Wang Y, Mu D, Qu L, Li R.** Hyperglycemia aggravates 6-hydroxydopamine-induced neuronal ferroptosis via SLC7A11-dependent pathway in diabetic PD rat model. CNS Neurosci Ther. 31(7): e70487, 2025.

43. **Wu K, Liu S.** Hippocampal dopamine as a key regulator for learning deficits in Parkinson's disease. Neural Regen Res. 19(6):1193–94, 2024.

**44. Meng J, Yan R, Zhang C, Bai X, Yang X, Yang Y, et al.** Dipeptidyl peptidase-4 inhibitors alleviate cognitive dysfunction in type 2 diabetes mellitus. Lipids Health Dis. 22(1):219, 2023.

**45. Dorszewska J, Prendecki M, Lianeri M, Kozubski W.** Molecular effects of L-DOPA therapy in Parkinson's disease. Curr Genomics. 15:11–17, 2014.

**46. Alrouji M, Al-Kuraishy HM, Al-Gareeb AI, Ashour NA, Jabir MS, Negm WA, Batiha GES.** Metformin role in Parkinson's disease: a double-sword effect.Mol Cell Biochem. 479(4):975-991, 2024.

**47. Barcia C, Ros CM, Annese V, Gomez A, Ros-Bernal F, Aguado-Llera D, et al.** IFN-γ signaling, with the synergistic contribution of TNF-α, mediates cell specific microglial and astroglial activation in experimental models of Parkinson's disease. Cell Death Dis. 2(4): e142, 2011.

**48. Khodir SA, Gaafar A, Mostafa B, Abd El-Aziz N, Elfakhrany A, Hassaan S, et al.** Sitagliptin mitigates scopolamine-induced neurocognitive deficits via activation of Nrf2/HO-1 pathway and improved mitochondrial activity. Egypt J For